Polymer Chemistry

ROYAL SOCIETY OF CHEMISTRY

PAPER

View Article Online
View Journal | View Issue

Cite this: *Polym. Chem.*, 2021, **12**, 1050

Main-chain liquid crystalline polymers bearing periodically grafted folding elements†

Gabriel Ogunsola Orodepo, [a] E. Bhoje Gowd [b] and S. Ramakrishnan *[a]

Received 3rd December 2020,
Accepted 23rd January 2021

DOI: 10.1039/d0py01661f

rsc.li/polymers

A series of main-chain liquid crystalline polymers (MCLCPs) carrying a biphenyl mesogen and a flexible alkylene spacer in the backbone was prepared; a unique feature of these polymers is that they have a non-mesogenic pendant segment, namely, an alkyl, PEG or fluoroalkyl segment, which is periodically located along the backbone. Due to the presence of these periodic substituents, the chain folds in a zigzag fashion, permitting the collocation of the mesogenic biphenyl units within one layer and the pendant segments in alternate layers of a lamellar morphology generated by these polymers. Most of the polymers were found to exhibit a stable smectic mesophase upon melting that appears to retain the folded chain conformation, which becomes disordered only after the isotropization transition. From the variation of the interlamellar spacing, estimated from SAXS studies, as a function of the pendant alkyl segment length, it was evident that the pendant segments adopted an extended all-*trans* conformation and these were fully interdigitated. Furthermore, by comparing the *d*-spacing of a sample that had longer alkylene backbone segments (C10 instead of C6), we were able to show that the linear variation remains valid for an increase in both the length of the pendant alkyl chain as well as that of the backbone alkylene segment. This observation serves as further evidence for the zigzag folded chain conformation adopted by this class of periodically substituted MCLCPs. Furthermore, the study also reveals the role of aromatic mesogens in enhancing the propensity to adopt this conformation and attain lamellar morphologies, wherein the dimensions are regulated by only the grafting density and the grafted segment length and not by the molecular weight of the polymer.

Introduction

Thermotropic main-chain liquid crystalline polymers (MCLCPs) can either be rigid-rod type or they could carry flexible spacers within the backbone; the former typically exhibit very high melting temperatures, whereas the latter may exhibit a wide range of melting points depending on the nature and length of the flexible backbone segments. Since the first report of wholly aromatic LC polyesters by Jackson and Kuhfuss,[1] two main strategies have been employed to reduce the melting temperatures of rigid-rod polymers; one is to include molecular kinks that perturb their linearity and the other is by the introduction of lateral substituents, which minimally influence their rod-like nature but serve as a bound solvent to lower the melting temperature substantially.[2–4] A majority of MCLCPs exhibit smectic-type mesophases, and the molecular origin of the layered structure has been the subject of numerous studies; these studies have helped reveal many interesting features of the organization of the polymer backbone and the lateral substituents in the mesophases that are formed. For instance, fully aromatic polyesters carrying a single alkyl substituent per repeat unit often form a biaxial nematic-type mesophase, wherein pairs of polymer chains organize laterally to form a sheet-like structure with disordered pendant alkyl chains on either side that provide the fluidity to the mesophase; however, those that carry two symmetrically disposed alkyl substituents per repeat unit form similar sheet-like assemblies but are built-up of laterally assembled single chains, whereas those with an even larger number of lateral substituents seldom form stable mesophases.[5–17] Interestingly, when the pendant alkyl chains are long (>12 C atoms), they often crystallize independently in the solid state, which upon melting leads to the formation of the fluid mesophase.[12,13] Inclusion of flexible spacers in the polymer backbone, on the other hand, leads to completely different organization of the chains in the mesophase, which is also of a smectic-type; however, the chains typically lay extended perpendicular to the

[a]*Department of Inorganic and Physical Chemistry, Indian Institute of Science, Bangalore 560012, India. E-mail: raman@iisc.ac.in*
[b]*Materials Science and Technology Division, CSIR-National Institute for Interdisciplinary Science and Technology (CSIR-NIIST), Trivandrum 695019, India*

†Electronic supplementary information (ESI) available: Detailed synthetic methods; NMR spectra of all intermediates, monomers and polymers; GPC curves of all polymers; SAXS data and their deconvolution studies. See DOI: 10.1039/d0py01661f

layer plane, with the mesogenic units lying either perpendicular (smectic A) or at an angle (semctic C) to the plane. A variety of flexible spacers, such as polymethylene,[17–27] oligoethylene oxide,[28–33] and oligosiloxane segments[34–36] have been incorporated within the backbone of the main-chain LCPs; oligosiloxane spacers have been found to reduce the phase transition temperatures most drastically and often lead to the formation of a nematic mesophase with wide temperature stability. In the cases where the pendant substituent is installed on the flexible spacer of the backbone, folding of the chain to exclude the pendant substituent is often seen;[37–43] this happens especially when a bulky pendant unit, such as a ferrocenyl[38,39] or phenyl unit,[40–43] is present. The layering of the rigid aromatic mesogenic units in such polymers having flexible backbone segments is often driven by steric and packing constraints. Thus, it is evident that several structural and topological attributes of MCLCPs play a crucial role in governing the nature and stability of the mesophase formed.

Some years ago, we began examining the possibility of causing chains to fold by installing immiscible pendant segments at periodic intervals along the polymer backbone (Scheme 1); for instance, locating PEG segments at periodic intervals along a polyethylene-like polyester made these periodically grafted amphiphilic copolymers (PGACs) fold in a zigzag fashion, thereby permitting both backbone and pendant segments to self-segregate and often crystallize independently, generating a lamellar morphology with sub-10-nm inter-lamellar spacing.[44–48] Building on these studies, we recently began exploring the possibility of enhancing the folding propensity of PGACs by the inclusion of mesogenic aromatic units, such as biphenyl or azobenzene, either within the pendant segment or within the polymer backbone; the presence of the rigid aromatic mesogens, we expected, would not only serve to enhance the tendency to fold but would also permit us to examine the possibility of regulating the nature of the mesophase formed. In our previous report, we examined the influence of the nature and length of the backbone segment in periodically spaced side-chain LCPs;[49] the studies revealed that when alkylene segments were present in the backbone, only nematic mesophases were formed, even though smectic-type layering was evident in the solid state. However, when polar flexible PEG segments were present in the backbone, lowering of the melting temperature and segment immiscibility drove the formation of smectic mesophases. In the present study, we examine the effect of *periodically installed non-mesogenic pendant segments* on the behavior of MCLCP-containing flexible spacers; three types of pendant segments, namely, alkyl, PEG and perfluoroalkyl segments, have been used to drive folding and cause layering of the biphenyl-based mesogenic units present in the backbone. We have examined the behavior of this series of polymers using DSC, PLM and X-ray diffraction studies; they reveal several interesting consequences of periodically located pendant segments on the LC properties of the polymers.

Experimental section

Materials

1-Iodo-1*H*,1*H*,2*H*,2*H*-perfluorodecane, PEG350 monomethyl ether, PEG550 monomethyl ether, sodium hydride (60% dispersion in mineral oil) and titanium(IV) isopropoxide were pur-

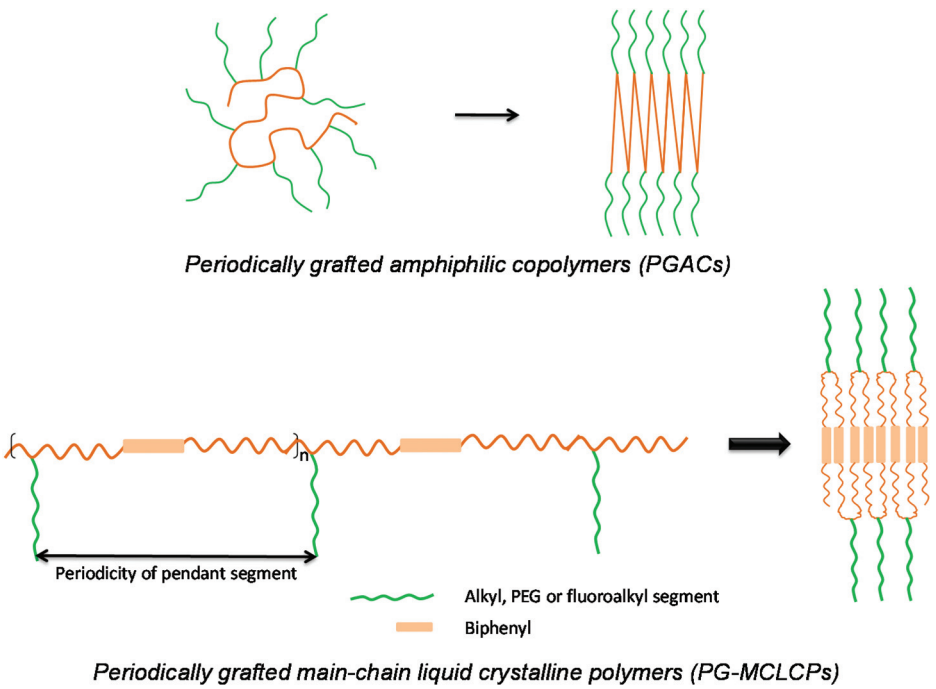

Scheme 1 Schematic depiction of segment immiscibility induced folding in PGACs and in mesogen bearing periodically substituted MCLCPs.

chased from Sigma-Aldrich Chemical company and used without further purification. 1-Eicosanol and 4,4′-dihydroxybiphenyl were bought from Tokyo Chemical Industry Co. (Japan) and used as such. 1-Bromooctane, diethyl malonate, dodecan-1-ol, cetyl alcohol, butan-1-ol, malonic acid, tosyl chloride and pyridine were sourced from other commercial sources (Thomas Baker, Spectrochem or SDFCL); all these were used as received. All the solvents used for the synthesis were distilled prior to use and dried if necessary, following the standard procedure.[50]

Characterization methods

NMR spectra of all synthesized compounds were recorded using a Bruker AV 400 MHz spectrometer in a suitable deuterated solvent, using tetramethylsilane (TMS) as an internal standard. GPC studies were carried out using a Viscotek TDA model 300 instrument with an RI detector; the separation of the polymers was achieved using a series of two PL gel mixed bed columns (300 × 7.5 mm) operated at 30 °C with THF as an eluent at a 1 ml min^{-1} flow rate. Molecular weights were estimated using a standard calibration curve prepared from data obtained from the RI detector using narrow polystyrene standards. Thermal characterization was performed using a PerkinElmer DSC 8000 instrument operating at a heating and cooling rate of 10° min^{-1} under a dry nitrogen atmosphere. Typically, 4–5 mg of the sample was used, and two heating (excluding the first heating) and cooling runs were performed to ascertain reproducibility in the measurement. SAXS/WAXS measurements were performed on a XEUSS instrument (XENOCS) operated at 50 kV and 0.60 mA power, fitted with Cu-Kα incident radiation (wavelength, λ = 1.54 Å). The fiber diagrams were recorded in transmission mode using an image plate system (Mar 345 detector), and data were processed with Fit2D software. The XEUSS system was equipped with a Linkam THMS 600 hot stage for variable temperature measurements. All the polarized optical microscopic (POM) studies were performed using an Olympus BX-51 polarizing microscope equipped with a Mettler Toledo (FP90 central processor) heater and an FP82HT hot stage. All the samples were first heated to melt where there was no birefringence and then slowly cooled at 5° min^{-1} to room temperature with a 2 min isotherm at each temperature to allow equilibration before capturing the images.

Typical polymerization procedure

The polymers were obtained by a melt-transesterification polymerization reaction.[51] The synthesis of the MCLCP having a pendant octyl (C8) chain length is described here as a representative example. 247.20 mg (0.908 mmol) of diethyl 2-octyl malonate and 350.78 mg (0.908 mmol) of 4,4′-bis(6-hydroxyhexyloxy) biphenyl were heated at 170 °C in the Kugelrohr apparatus under moderate vacuum (~300 mm of Hg) to obtain a homogeneous mixture. The melt was cooled to ambient temperature, and 3.00 mg (0.5 wt% w.r.t. total monomer weight) of titanium(IV) isopropoxide was added, as 235 μL of a toluene solution, to the mixture as a catalyst. The mixture was heated at 170 °C under a reduced pressure of 100 mm Hg for 4 h, after which the temperature was increased to 180 °C and high vacuum (<1 Torr) was applied for another 2 h. When it was observed that the melt had become highly viscous, as was evident from the sluggish rotation of the spin bar, the melt was cooled to room temperature and the polymer was dissolved in a solvent mixture of *p*-chlorophenol and 1,1,2,2-tetrachloroethane (60 : 40 v/v) at 120 °C. The solution was diluted with $CHCl_3$ and filtered to remove any insoluble portion. The polymer was isolated after subjecting to dissolution twice in chloroform and precipitation from methanol. It was further purified by refluxing in methanol, followed by centrifugation and drying to constant weight in an oven. The polymer was obtained in 82% yield (420 mg).

Results

The polymers were prepared from suitably derivatized diethylmalonate (A) and a diol (B), bearing a mesogenic biphenyl unit (Scheme 2), under standard melt transesterification conditions using titanium tetraisopropoxide as the catalyst (see the ESI† for details). The structure of the polymers was confirmed by ^{1}H NMR spectroscopy; a representative stack plot of the spectra of the polymer bearing a C16 aliphatic pendant segment (MC-BP6-C16) and those of the corresponding monomers is shown in Fig. 1.

A comparison of the spectra of the monomers with that of the polymer reveals the expected downfield shift of the methylene protons (–C**H**$_2$OH) at ~3.65 ppm, in the diol monomer, to ~4.20 ppm in the polymer (dashed line in Fig. 1). A weak peak

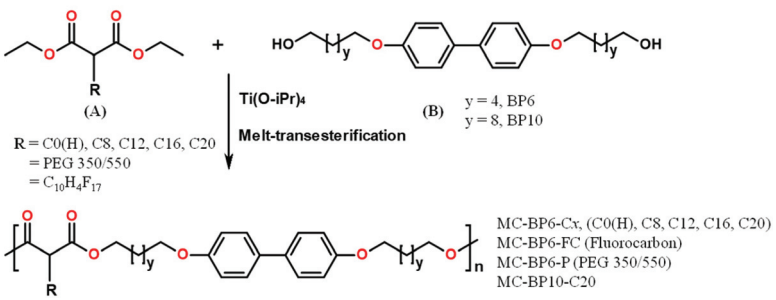

Scheme 2 Synthesis and structures of periodically grafted MCLCPs.

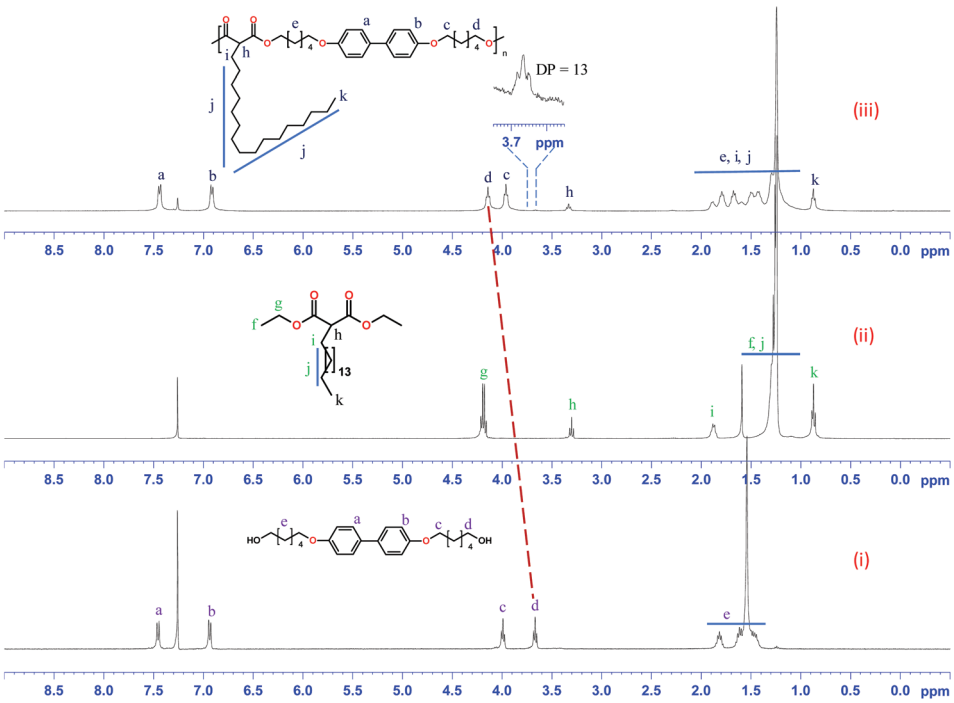

Fig. 1 ^{1}H NMR spectra (in $CDCl_3$) of biphenyl containing diol (i); C16-DEM monomer (ii); and the corresponding polymer, MC-BP6-C16 (iii). The expanded region reveals the CH_2–OH end-group; the DP_n was estimated, assuming equimolar amounts of the two types of end-groups.

Table 1 Properties of the MCLCPs bearing biphenyl mesogens with different periodically located pendant segments. The heating and cooling scans were performed at 10 °C min^{-1}

Polymers	Pendant group	M_n, GPC	DP	T_m (°C)	ΔH_m (J g^{-1})	T_i (°C)	ΔH_i (J g^{-1})	ΔH_i (norm)
MC-BP6-H	H	4600	10	126	22.8	144	18.8	24.1
MC-BP6-C8	C_8H_{17}	11 400	20	71	5.8	100	21.0	33.9
MC-BP6-C12	$C_{12}H_{25}$	20 900	34	87	7.8	115	26.6	46.7
MC-BP6-C16	$C_{16}H_{33}$	21 000	31	88	42.3	124	28.7	55.2
MC-BP6-C20	$C_{20}H_{41}$	29 200	40	83	49.7	123	26.5	55.2
MC-BP6-PEG 350	MPEG350	16 000	21	84	26.1	—	—	—
MC-BP6-PEG 550	MPEG550	14 500	15	76	23.1	—	—	—
MC-BP6-FC	$C_{10}H_5F_{17}$	11 000	12	130	3.5	178	16.8	43.1
MC-BP10-C20	$C_{20}H_{41}$	28 200	33	60	18.4	110	53.8	97.8

corresponding to the residual CH_2OH end-group is also seen, which was used to estimate the degree of polymerization, assuming that equimolar amounts of both end-groups are present in the sample; in this case, MC-BP6-C16, it gave a value of ~13. The spectra of all other polymers are provided in the ESI.† In the PEG-containing samples, the end-group signals overlapped with other peaks and hence their DP values could not be estimated. However, the GPC analyses of all the samples were carried out and the molecular weights were found to be moderate; these are listed in Table 1.

Thermal analysis

The DSC thermograms of the MCLCPs carrying pendant alkyl chains are shown in Fig. 2. In all samples, multiple transitions were observed, although in some cases the peaks were weak; the reproducibility of the thermograms was established by confirming the overlap of the second and third heating/cooling scans. For comparison, the thermogram of the polymer without a pendant substituent (MC-BP6-C0) was also provided; in most polymers (C0–C16), the peak corresponding to the isotropization transition (T_i) was relatively more intense, suggesting the formation of smectic type mesophases. It was also observed that the melting enthalpies (ΔH_m) of C16 and C20 samples were significantly larger than those of C8 and C12; this is suggestive of independent crystallization of the pendant chains in the former two samples. The postulated zigzag folding, as depicted in Scheme 1, would segregate the pendant segment and the backbone to facilitate crystallization; if this were the case, the melting temperature (T_m) could reflect the disordering of pendant alkyl groups, whereas the isotropization temperature (T_i) would be associated with the complete disordering of the folded chains. It is well known

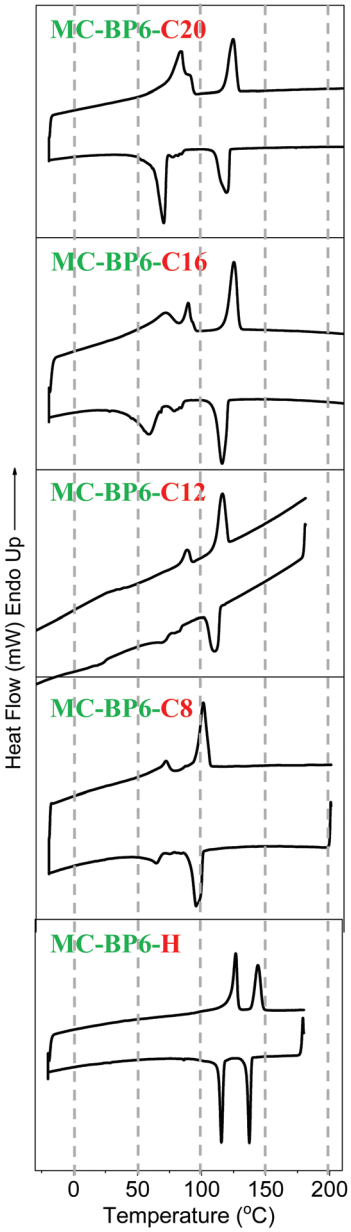

Fig. 2 DSC thermograms of MCLCPs carrying periodically installed pendant alkyl chains of different lengths.

that side-chain crystallization in polymers occurs only when the length of the pendant alkyl chain is at least 12 carbon long;[52] furthermore, such segregation and melting of pendant alkyl substituents have also been observed in the case of laterally substituted rigid-rod polyesters, and similar disordering of lateral alkyl chains is postulated upon the formation of the fluid mesophase.[12–15] To gain further insight, the isotropization enthalpy is normalized with respect to the mesogen segment (–C6–O–biphenyl–O–C6–) that straddles adjacent malonate units and these values are listed in Table 1; the mesogen-normalized isotropization enthalpies are likely to reflect the effectiveness of the decoupling of the backbone and pendant chains. The normalized isotropization enthalpies of C12, C16 and C20 fall in the range 47–55 J g^{-1}; interestingly, the values for C0 and C8 are significantly smaller. Overall, these observations appear to suggest that the effectiveness of zigzag folding and decoupling of the pendant alkyl chains and the backbone is better with the longer alkyl chains (≥C8).

In the polymers carrying pendant fluoroalkyl (FC) segments, the isotropization temperature (T_i) was significantly higher (Fig. 3), even higher than that of the unsubstituted analogue (MC-BP6-C0). This is along expected lines as the fluoroalkyl segments are more rigid and pack more effectively, thereby increasing the transition temperatures; similar observations were also made in our earlier studies on fluoro-PGACs.[46] On the other hand, pendant PEG chains significantly lowered the melting/isotropization temperatures and the corresponding polymers did not form a smectic mesophase but rather a nematic one; thus, MC-BP6-PEG550 exhibited a narrow LC phase, whereas MC-BP6-PEG350 was monotropic, which is again consistent with the fact that PEG segments are in a disordered state, possibly adopting a coiled conformation. It may be important to recall here that when the backbone adopts a zigzag folded conformation, the cross-sectional area available to the pendant segments at the folding interface is equal to that of two backbone alkylene segments, since the pendant segments are equally distributed on either side of the

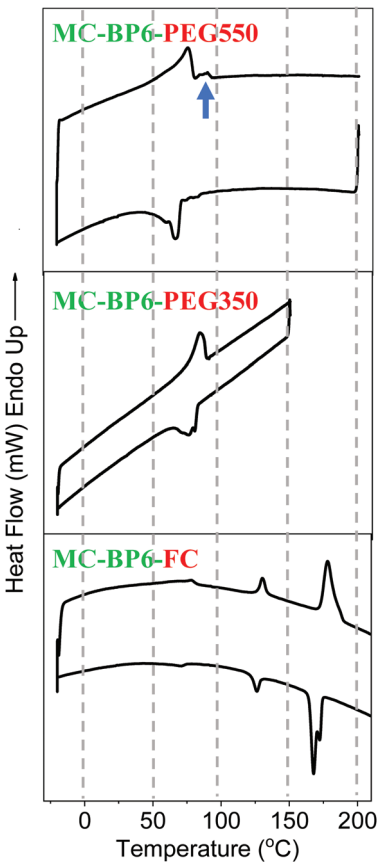

Fig. 3 DSC thermograms of MCLCPs with biphenyl mesogens and periodically grafted pendant PEG or fluoroalkyl segments. The arrow indicates a weak transition.

folded chains; therefore, there is ample space available to accommodate all three types of pendant segments in the folded conformation. Thus, although installation of the pendant PEG segment may drive zigzag folding and microphase separation, it does not necessarily lead to the formation of a stable ordered mesophase; whereas in the fluoroalkyl (FC) substituted sample, a smectic mesophase appears to be formed over a fairly wide temperature window of ~50° C. In summary, the DSC studies suggest that the introduction of pendant non-mesogenic segments at periodic intervals leads to the reduction of both melting and clearing transition temperatures when compared with the model polymers having no pendant units, with the exception of the fluoroalkyl pendant segment. This is generally in agreement with earlier studies by Angeloni and co-workers.[37]

Polarized optical microscopic studies

In order to confirm the formation of a mesophase, thin films of the samples were observed under a polarized optical microscope as a function of temperature; typically, the samples are heated above the isotropization temperature (T_i) and then cooled slowly. In the isotropic state, the sample appears completely dark under crossed polarizers; upon transition into a mesophase, birefringent patterns, which are sensitive to shear, are seen, revealing its fluid nature (see Fig. 4). Upon cooling further, crystallization occurs, causing the birefringent patterns to freeze and become unresponsive to shear. Although the patterns are not as well developed as in small-molecule LCs, the mosaic texture suggests a smectic-type mesophase. Due to the highly viscous nature of the melt, the birefringent patterns are often less well developed in polymers; X-ray diffraction studies to confirm the nature of the mesophases are discussed in the next section.

X-ray scattering studies

As stated earlier, immiscibility-driven chain folding could lead to effective segregation of the rigid mesogen-containing backbone from the more flexible pendant chains; and in the case of the fluoroalkyl and PEG segments, polarity differences may further drive the self-segregation. To examine the self-segregation and microphase separation, X-ray scattering measurements in the small-angle and wide-angle regions were recorded as a function of temperature (Fig. 5). At room temperature, the SAXS profiles of the alkyl substituted MCLCPs revealed a single sharp peak in all cases (Fig. S6†) and weak higher order peaks in a few cases, suggesting the presence of lamellar ordering; the absence of well-developed higher order peaks suggests that the ordering is not over extended length scales. Taking the single peak as the 001 reflection, the interlamellar spacing was estimated; the values varied between 2.54 nm and 5.15 nm, and these are listed in Fig. S6.† Based on the scattering profiles as a function of temperature (Fig. 5), the following key observations for the series, MC-BP6-C*n*, can be made: (a) the sharp peak in the small-angle region reflecting the lamellar (smectic) ordering is retained even after the first melting transition (T_m) and it disappears only beyond the second (isotropization, T_i) transition; (b) in the wide-angle region, the two peaks (one broad and another sharp), present in the crystalline state (at RT), transforms to a single sharper peak (at ~20.4°) upon the formation of the mesophase; and (c) during cooling, the sharp wide-angle peak appears first, along with the intense peak in the small-angle region, and upon further cooling the initial scattering profile is restored. The broad peak centered at 20.4° (2θ) and the sharper one at 23.5° (2θ) correspond to *d*-spacings of 4.35 Å and 3.78 Å, respectively; as assigned earlier,[49] the 3.78 Å peak reflects the spacing between adjacent biphenyl mesogens in the crystalline state, whereas the broad 4.35 Å peak reflects the average distance between the alkyl chains. Although these two peaks could alternatively reflect the formation of a 3-dimensionally ordered array of biphenyl units, such as in a smectic E-type arrangement, spatial correlation between adjacent layers in polymeric systems would be more difficult given that the pendant segments of the folded chains will need to serve as a bridge for effective correlation. Upon melting, the newly formed sharp peak possibly reflects the spacing between well-ordered biphenyl units within the mesophase; the larger inter-mesogen spacing of ~4.4 nm, in the mesophase, is to be expected and is

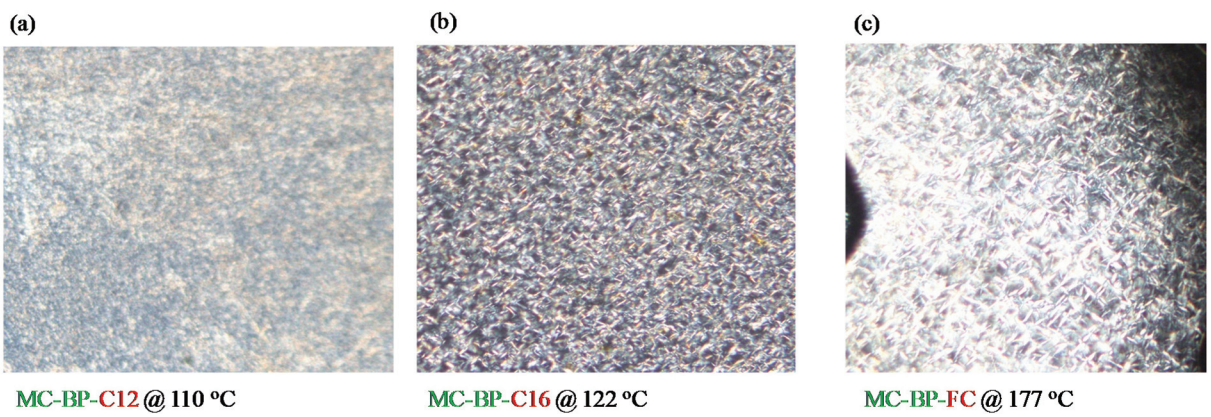

Fig. 4 POM images of selected MCLCPs taken at indicated temperatures during cooling from the melt; the sample identity and the temperature at which the images were taken for (a), (b) and (c) are indicated below each photograph.

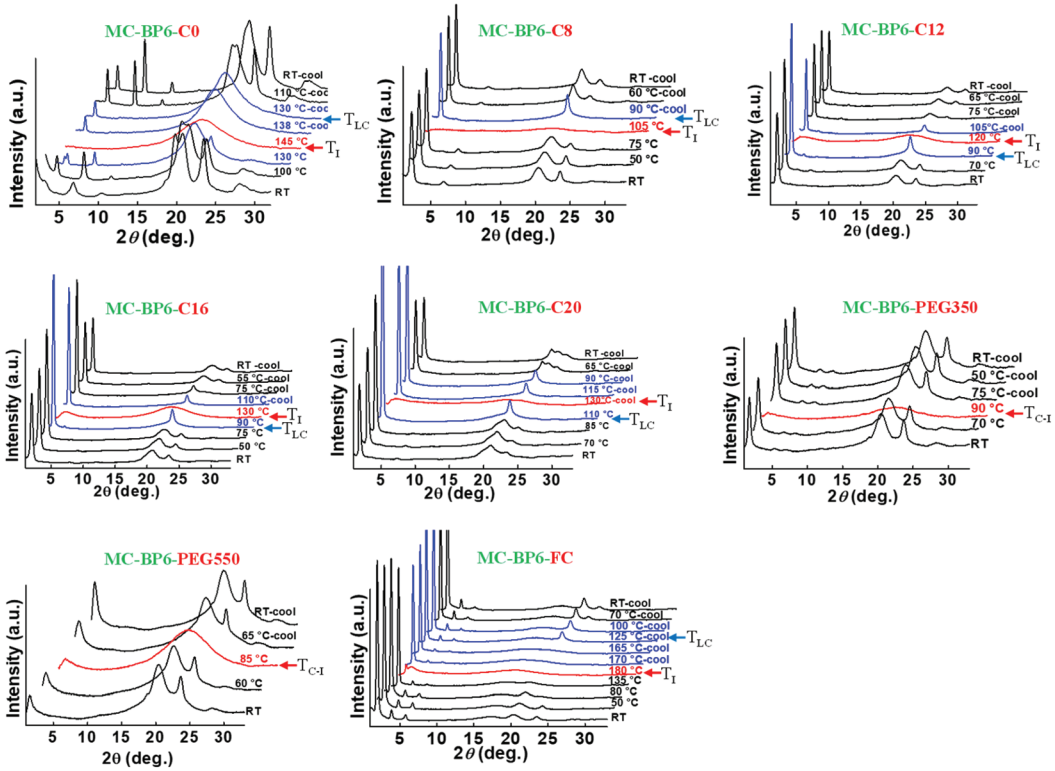

Fig. 5 Variable temperature X-ray scattering profiles of MCLCPs with periodically located pendant segments.

similar to the values earlier reported.[53] The presence of a single sharp peak upon melting to form the mesophase is reminiscent of the hexatic-B phase, wherein there is local ordering of the mesogens within the layer;[54,55] however, when the mesophase is cooled, crystallization involving other segments in the chain appears to impede this ordering. These observations clearly confirm the formation of a layered smectic-type mesophase in all MC-BP6-C*x* samples, which is consistent with the DSC data. However, in the samples with pendant PEG segments, no clear evidence of a smectic mesophase is seen; MC-BP6-PEG350 directly transforms to an isotropic melt, while in MC-BP6-PEG550, weak layering could be present. The variation in MC-BP6-FC, however, is similar to that seen in the alkyl-substituted samples; an improved ordering of the biphenyl mesogens is observed upon formation of the mesophase.

Effect of size of the backbone spacer segment

Thus far, we have examined the effect of periodic pendant substituents on the behavior MCLCPs; it is noted that even with a C20 pendant alkyl chain, the LC behavior is retained. In order to investigate the effect of the length of the backbone spacer on the mesomorphic properties, a polymer carrying a longer backbone segment, namely, MC-BP10-C20, was prepared (Scheme 2); here, the backbone segment length was increased from C6 to C10 while retaining a constant pendant C20 segment.

The DSC plot, shown in Fig. 6, reveals the presence of multiple transitions, both during heating and cooling runs; a comparison of these data with MC-BP6-C20 reveals a significant decrease in both the melting (T_m) and isotropization temperatures (T_i). However, observing the sample under a polarizing light microscope revealed that the sample does not melt as it goes past the first two weak peaks and directly transforms to an isotropic liquid above 110 °C; this suggests that the low-temperature peaks reflect some kind of crystal–crystal transition. Variable-temperature X-ray scattering measurements also confirm these observations; as is evident from Fig. 6, the pattern changes very little until it transforms into an isotropic phase. However, on careful observation, one can observe an enhancement in the lamellar ordering during heating at 65 °C, as reflected by the increase in the intensity of the higher order peaks; likewise, there is a sharpening of the wide-angle peaks as well at this temperature (for details, see Fig. S7†). Thus, the inclusion of C10 spacers in the backbone, along with a C20 pendant segment, dilutes the mesogen volume fraction and appears to preclude the formation of a mesophase;[56,57] the increase in the backbone spacer clearly does not hinder the lamellar ordering in the solid state.

Discussions

The polymers described in this study can be analyzed from two different perspectives: one is the effect of periodically installed non-mesogenic segments in a spacer containing MCLCPs, whereas the second is the influence of rigid aromatic mesogens, such as biphenyl, on the propensity of the polymer to form a microphase separated lamellar morphology *via*

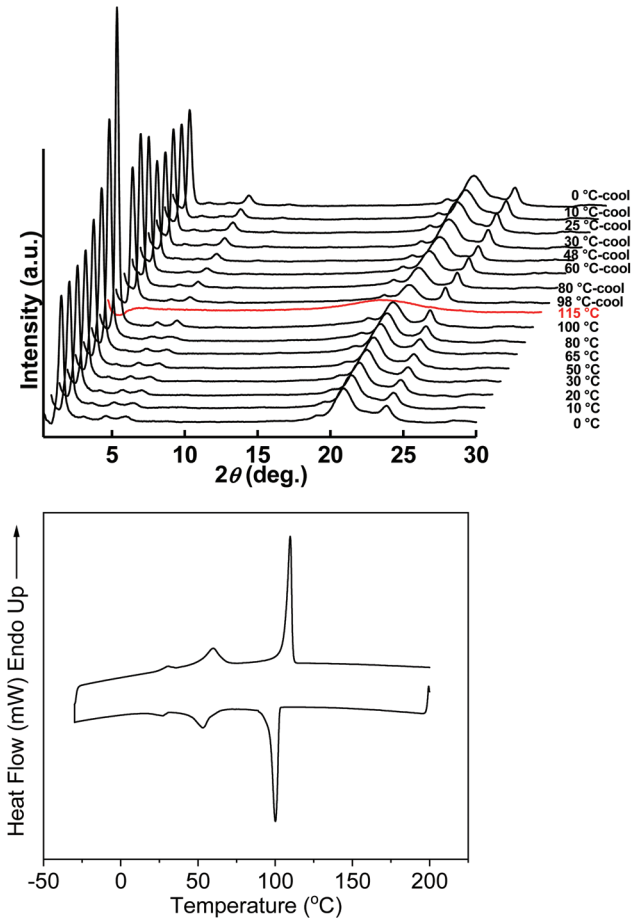

Fig. 6 DSC thermogram (bottom) and variable temperature X-ray scattering profiles (top) of MC-BP10-C20.

zigzag folding of the chain. The zigzag folding of the chain, as depicted in Scheme 3, would result in a layered morphology wherein the biphenyl mesogens are organized within one layer and the pendant segments in alternate layers. To fully understand this organization and assess the inter-digitation of the pendant segments, the *d*-spacing was plotted as a function of the pendant alkyl segment length and is shown in Fig. 7. In addition, the sample with a longer alkylene spacer in the backbone, namely, MC-BP10-C20, was also included in the plot; this was done considering that it contained 8 additional methylene units, even though these were present in the backbone. The linear variation seen across the entire range of samples is rather interesting; importantly, the slope of the variation is estimated to be 0.128 nm, which is close to the expected increase of 0.127 nm per methylene unit for an extended all-*trans* conformation.[48] The observation that the linear variation holds across both sample categories, immater-

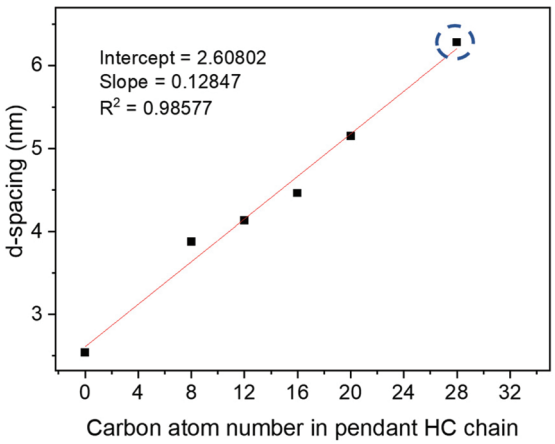

Fig. 7 Plot of variation of *d*-spacing as a function of carbon atom number (*x*) in the pendant alkyl segment for the series, MC-BP6-C*x*. The encircled data point is for sample MC-BP10-C20, which was notionally considered as one that includes 8 additional methylene units, although these units were included in the main-chain and not the pendant segment.

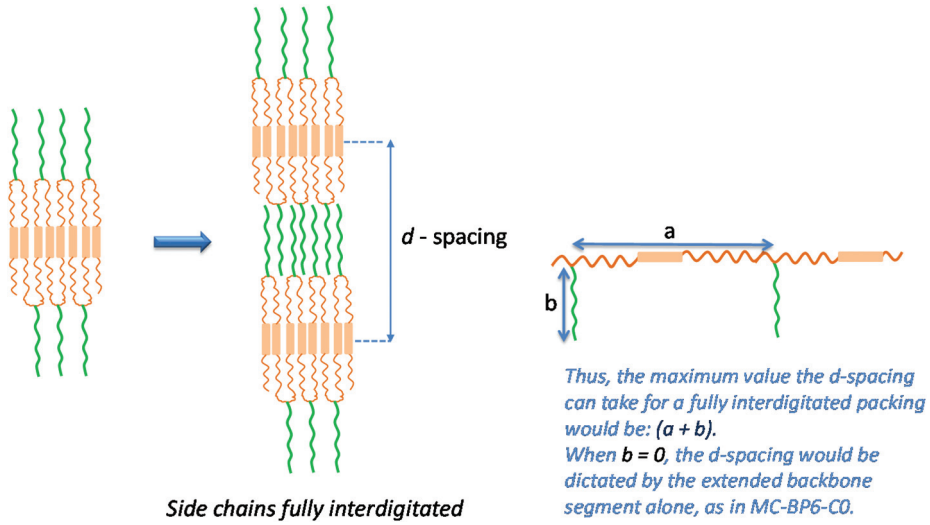

Scheme 3 Schematic depiction of the proposed zigzag folded polymer and the consequent formation of a lamellar morphology.

ial of whether the methylene segment is included within the pendant alkyl chain or in the backbone alkylene segment, serves as a reconfirmation of the zigzag folded conformation adopted by the polymer chains; as depicted in Scheme 3, the *d*-spacing could have a maximum value equal to the sum of the pendant and backbone segment lengths, in their extended conformations. Furthermore, the increment of 0.128 nm per methylene also suggests that the pendant segments are extended and fully inter-digitated as depicted in the schematic. Curiously, the polymer without any pendant segment, namely, MC-BP6-C0, also exhibits a spacing that is consistent with the linear variation; here, it is important to note that this does not necessarily imply that MC-BP6-C0 will also have adopted a zigzag folded conformation since even if the polymer chains lay extended perpendicular to the layers formed by the biphenyl mesogens, the inter-layer spacing would be the same (see Fig. S8†). Computational studies of a model dimer (Fig. S11†) were not conclusive; they appeared to suggest that a slightly bent conformation is preferred; however, the minimum energy structure was not the completely folded form that brings the aromatic mesogens in close proximity, as is the case with the zigzag folded chains. Hence, unequivocal conclusions concerning the conformation in the case of MC-BP6-C0 were not possible.

Conclusions

This study sought to understand the effect of the nature and length of periodically located pendant substituents, such as alkyl, PEG and fluorocarbon substituents, on the mesomorphic properties of a series of main-chain liquid crystalline polymers carrying biphenyl mesogens along with flexible alkylene spacers. Keeping the backbone segment fixed, upon increasing the length of the periodically located pendant alkyl chain from C0 to C20 in the series MC-BP6-C*x*, it was observed that the inter-lamellar spacing varied linearly with the pendant chain length; a slope of 0.128 nm was consistent with an extended all-*trans* conformation adopted by the alkylene segments. Remarkably, the *d*-spacing of a sample where the backbone alkylene segment length was increased from C6 to C10, namely, in MC-BP10-C20, was also in accordance with this linear fit, suggesting that an increase in either of the chain segments, backbone or pendant, affected the spacing in a consistent manner; this reaffirmed the proposed zigzag folded conformation that causes the segregation of the backbone and pendant segments and leads to the lamellar morphology in the solid state. However, the polymer with the longer C10 alkylene backbone segment did not exhibit a stable mesophase, evidently because of the mesogen dilution effect. On the other hand, installation of the pendant fluorocarbon segment did not influence the general characteristics considerably, although it led to a substantial increase in the transition temperatures; however, pendant PEG segments, despite driving segregation and lamellar ordering, destabilized the mesophase. In summary, tailoring the polymer architecture to control the type of mesophase formed in MCLCPs is a complex proposition; although, the principle of segregation of the mesogen-carrying backbone from the pendant segments leads to a layered organization in the solid state and, in many cases, also to the formation of smectic mesophases, this is not an assured consequence, as was seen with the polymers bearing pendant PEG segments, which did not reveal a very stable mesophase. Evidently, the interplay of the strength of interactions within the segregated domains and the segment disordering temperatures plays a crucial role in governing the mesophase stability. However, the inclusion of a rigid aromatic mesogenic unit within the backbone appears to enhance the immiscibility between the backbone segment and the pendant alkyl chains, thereby driving self-segregation; such an effect is inferred in an earlier study on block copolymers by Zhou *et al.*[58] It is relevant to recognize that the segregation of aromatic and aliphatic segments in small molecular systems is often the basis for the formation of smectic and discotic mesophases.[59] Thus, from the viewpoint of enhancing the folding-induced formation of lamellar morphologies in periodically grafted copolymers, the inclusion of specific interactions within either the backbone/pendant segments, such as π-stacking, H-bonding, *etc.*, could serve as an interesting strategy to realize ultrasmall domain sizes.

Conflicts of interest

There are no conflicts of interest to declare.

Acknowledgements

The authors would like to thank the Department of Science and Technology, New Delhi, for the award of the J C Bose fellowship (2016–2021) to SR. The authors would also like to thank Mr Amal Raj, NIIST, Thiruvananthapuram for carrying out XRD measurements, Mr Arun Kumar Gayen for assistance with the computational studies and Professor Sandeep Kumar and Dr Aswath Gowda of Raman Research Institute, Bangalore, for PLM measurements. The authors would also like to thank Dr Krishna Prasad and Dr Shankar Rao from CeNS, Bangalore, for some insightful discussions concerning the mesophase structure. GOO would like to thank the Indian Institute of Science for the fellowship.

References

1 W. J. Jackson and H. F. Kuhfuss, *J. Polym. Sci., Polym. Chem. Ed.*, 1976, **14**, 2043–2058.
2 M. Ballauff, *Angew. Chem., In. Ed. Engl.*, 1989, **28**, 253–396.
3 J.-I. Jin and C.-S. Kang, *Prog. Polym. Sci.*, 1997, **22**, 937–973.
4 H. Han and P. K. Bhowmik, *Prog. Polym. Sci.*, 1997, **22**, 1431–1502.
5 H.-R. Dicke and R. W. Lenz, *J. Polym. Sci., Polym. Chem. Ed.*, 1983, **21**, 2581–2588.
6 J. Majnusz, J. M. Catala and R. W. Lenz, *Eur. Polym. J.*, 1983, **19**, 1043–1046.

7 W. R. Krigbaum, H. Hakemi and R. Kotek, *Macromolecules*, 1985, **18**, 965–973.
8 M. Ballauff, *Macromolecules*, 1986, **19**, 1366–1374.
9 M. Ballauff, *Makromol. Chem., Rapid Commun.*, 1986, **7**, 407–414.
10 M. Ballauff and G. F. Schmidt, *Makromol. Chem., Rapid Commun.*, 1987, **8**, 93–97.
11 M. Ballauff and G. F. Schmidt, *Mol. Cryst. Liq. Cryst.*, 1987, **147**, 163–177.
12 R. Stern, M. Ballauff, G. Lieser and G. Wegner, *Polymer*, 1991, **32**, 2096–2105.
13 H. R. Kricheldorf and A. Domschke, *Macromolecules*, 1996, **29**, 1337–1344.
14 J. Watanabe, B. R. Harkness, M. Sone and H. Ichimura, *Macromolecules*, 1994, **27**, 507–512.
15 K. Fu, T. Nematsu, M. Sone, T. Itoh, T. Hayakawa, M. Ueda, M. Tokita and J. Watanabe, *Macromolecules*, 2000, **33**, 8367–8370.
16 D. Acierno, E. Amendola, S. Concilio, R. Fresa, P. Iannelli and P. Vacca, *Macromolecules*, 2000, **33**, 9376–9384.
17 K. Clausen, J. Kops, K. Rasmussen, K. H. Rasmussen and J. Sonne, *Macromolecules*, 1987, **20**, 2660–2664.
18 J. Watanabe and M. Hayashi, *Macromolecules*, 1989, **22**, 4083–4088.
19 J. Watanabe, M. Hayashi, S. Kinoshita and T. Niori, *Polym. J.*, 1992, **24**, 597–601.
20 E. Pérez, Z. Zhen, A. Bello, R. Benavente and J. M. Pereña, *Polymer*, 1994, **35**, 4794–4798.
21 C. D. Han, S. Chang and S. S. Kim, *Macromolecules*, 1994, **27**, 7699–7712.
22 A. Bello, J. M. Pereña, E. Pérez and R. Benavente, *Macromol. Symp.*, 1994, **84**, 297–306.
23 M. Tokita, K. Osada, M. Yamada and J. Watanabe, *Macromolecules*, 1998, **31**, 8590–8594.
24 D. Acierno, S. Concilio, P. Iannelli and P. Vacca, *Macromolecules*, 2000, **33**, 9688–9695.
25 D. Acierno, E. Amendola, R. P. Fresa, P. Iannelli and P. Vacca, *Polymer*, 2000, **41**, 7785–7792.
26 E. Pérez, G. Todorova, M. Krasteva, J. M. Pereña, A. Bello, M. M. Marugán and M. Shlouf, *Macromol. Chem. Phys.*, 2003, **204**, 1791–1799.
27 A. S. Kuenstler, K. D. Clark, J. Read de Alaniz and R. C. Hayward, *ACS Macro Lett.*, 2020, **9**, 902–909.
28 P. Meurisse, C. Noel, L. Monnerie and B. Fayolle, *Br. Polym. J.*, 1981, **13**, 55–63.
29 K. Limura, N. Koide, R. Ohta and M. Takeda, *Makromol. Chem.*, 1981, **182**, 2563–2568.
30 K. Limura, N. Koide, H. Tanabe and M. Takeda, *Makromol. Chem.*, 1981, **182**, 2569–2575.
31 G. Galli, E. Chiellini, C. K. Ober and R. W. Lenz, *Makromol. Chem.*, 1982, **183**, 2693–2708.
32 W. Volksen, D. Y. Yoon and P. M. Cotts, *Macromolecules*, 1989, **22**, 3846–3850.
33 A. Martínez-Goméz, E. Pérez and A. Bello, *Colloid Polym. Sci.*, 2010, **288**, 859–867.
34 C. Aguilera, J. Bartulin, B. Hisgen and H. Ringsdorf, *Makromol. Chem.*, 1983, **184**, 253–262.
35 F. Diaz, L. H. Tagle, N. Valdebenito and C. Aguilera, *Polymer*, 1993, **34**, 418–422.
36 A. B. Samui, S. Pandey and S. P. Mishra, *RSC Adv.*, 2015, **5**, 68351–68355.
37 A. S. Angeloni, D. Caretti, C. Carlini, E. Chiellini, G. Galli, A. Altomare, R. Solaro and M. Laus, *Liq. Cryst.*, 1989, **4**, 513–527.
38 G. Wilbert and R. Zentel, *Macromol. Chem. Phys.*, 1996, **197**, 3259–3268.
39 G. Wilbert, S. Traud and R. Zentel, *Macromol. Chem. Phys.*, 1997, **198**, 3769–3785.
40 A. Vix, W. Stocker, M. Stamm, G. Wilbert, R. Zentel and J. P. Rabe, *Macromolecules*, 1998, **31**, 9154–9159.
41 R. Yang, L. Chen, C. Ruan, H.-Y. Zhong and Y.-Z. Wang, *J. Mater. Chem. C*, 2014, **2**, 6155–6164.
42 H.-Y. Zhong, L. Chen, R. Yang, Z.-Y. Meng, X.-M. Ding, X.-F. Liu and Y.-Z. Wang, *J. Mater. Chem. C*, 2017, **5**, 3306–3314.
43 R. Yang, L. Ding, W. Chen, L. Chen, X. Zhang and J. Li, *Macromolecules*, 2017, **50**, 1610–1617.
44 R. K. Roy, E. B. Gowd and S. Ramakrishnan, *Macromolecules*, 2012, **45**, 3063–3069.
45 S. Chanda and S. Ramakrishnan, *Macromolecules*, 2016, **49**, 3254–3263.
46 J. Mandal, S. Krishna Prasad, D. S. S. Rao and S. Ramakrishnan, *J. Am. Chem. Soc.*, 2014, **136**, 2538–2545.
47 R. Sarkar, E. B. Gowd and S. Ramakrishnan, *Polym. Chem.*, 2019, **10**, 1730–1740.
48 R. Sarkar, E. B. Gowd and S. Ramakrishnan, *Polym. Chem.*, 2020, **11**, 4143–4154.
49 G. O. Orodepo, E. B. Gowd and S. Ramakrishnan, *Macromolecules*, 2020, **53**, 8775–8786.
50 D. D. Perrin, W. L. F. Armarego and D. R. Perrin, *Purification of Laboratory Chemicals*, Pergamon Press, 1980.
51 B. Reck and H. Ringsdorf, *Makromol. Chem., Rapid Commun.*, 1985, **6**, 291–299.
52 J. L. Lee, E. M. Pearce and T. K. Kwei, *Macromolecules*, 1997, **30**, 6877–6883.
53 R. Zentel and G. R. Strobl, *Makromol. Chem.*, 1984, **185**, 2669–2676.
54 G. Albertini, E. Fanelli, S. Melone, F. Rustichelli and G. Torquati, *Solid State Commun.*, 1984, **49**, 1143–1146.
55 E. Górecka, L. Chen, W. Pyżuk, A. Krówczyński and S. Kumar, *Phys. Rev. E*, 1994, **50**, 2863–2867.
56 A. M. Donald and A. H. Windle, *Liquid Crystalline Polymers*, Cambridge University Press, Cambridge, U. K., 1992, ch. 5, p. 159.
57 C. K. Ober, J.-I. Jin, Q. Zhou and R. W. Lenz, in *Liquid Crystal Polymers I. Advances in Polymer Science*, ed. N. A. Platé, Springer, Berlin, Heidelberg, 1984, vol. 59.
58 S. X. Zhou, D. W. Janes, C. B. Kim, C. G. Willson and C. J. Ellison, *Macromolecules*, 2016, **49**, 8332–8340.
59 D. Demus, J. W. Goodby, G. W. Gray, H. W. Spiess and V. Vill, *Handbook of Liquid Crystals*, WILEY-VCH, Weinheim, 1998, vol. 2A.